Optimal water allocation of the Zayandeh-Roud Reservoir in Iran based on inflow projection under climate change scenarios

Fatemeh Saedi, Azadeh Ahmadi and Karim C. Abbaspour

ABSTRACT

The impact of climate change on water availability has become a significant cause for concern in the Zayandeh-Roud Reservoir in Iran and similar reservoirs in arid regions. This study investigates the climate change impact on water supply and availability in the Zayandeh-Roud River Basin. For better management, the Soil & Water Assessment Tool (SWAT) was used to develop a hydrologic model of the basin. The model was then calibrated and validated for two upstream stations using the Sequential Uncertainty Fitting (SUFI-2) algorithm in the SWAT-CUP software. The impact of climate change was modeled by using data derived from five Inter-Sectoral Impact Model Intercomparison Project general circulation models under four Representative Concentration Pathways (RCPs). For calibration (1991–2008), the Nash–Sutcliffe efficiency (NSE) values of 0.75 and 0.61 at the Ghaleshahrokh and Eskandari stations were obtained, respectively. For validation (2009–2015), the NSE values were 0.80 and 0.82, respectively. The reservoir inflow would probably reduce by 40–50% during the period of 2020–2045 relative to the base period of 1981–2006. To evaluate the reservoir's future performance, a nonlinear optimization model was used to minimize water deficits. The highest annual water deficit would likely be around 847 MCM. The lowest reservoir reliability and the highest vulnerability occurred under the extreme RCP8.5 pathway.

Key words | general circulation models, reservoir performance index, SUFI-2, SWAT

HIGHLIGHTS

- The Soil & Water Assessment Tool model was used to simulate an arid watershed in Iran.
- The reservoir inflow will probably reduce significantly under climate change scenarios.
- The reservoir will be vulnerable and unreliable in supplying water in the future.
- The highest annual water deficit of 847 MCM is expected under the extreme climate change scenario.

Fatemeh Saedi
Azadeh Ahmadi (corresponding author)
Department of Civil Engineering,
Isfahan University of Technology,
Isfahan 84156-83111,
Iran
E-mail: *aahmadi@cc.iut.ac.ir*

Karim C. Abbaspour
Eawag, Swiss Federal Institute of Aquatic Science and Technology,
P.O. Box 611, CH-8600 Dübendorf,
Switzerland

doi: 10.2166/wcc.2021.219

GRAPHICAL ABSTRACT

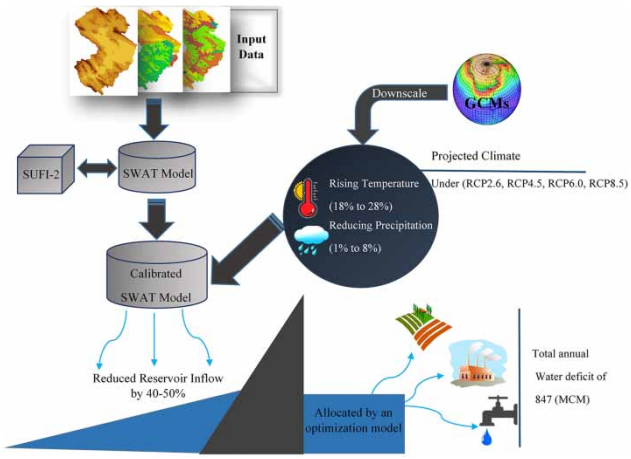

INTRODUCTION

Water resources in developing countries are experiencing significant pressures due to the growing population, increasing demands, non-sustainable water consumption patterns, and poor management practices (Vorosmarty *et al.* 2000; Marin *et al.* 2020). The changes expected to occur in the coming decades will challenge or even jeopardize already constructed water schemes' performance. They will increase the pressure on water resources. The hydrologic changes resulting from climate change will affect the planning, design, and operation of water resource systems. Developing water schemes based on present conditions without considering possible future changes could increase water resource pressure in the coming period. Therefore, it is of utmost importance to consider these changes in the future design and management of water supply systems (Ashofteh *et al.* 2015). Most climate change studies reveal a significant impact on available water resources on global and regional scales (Vorosmarty *et al.* 2000; Abbaspour *et al.* 2009; Faramarzi *et al.* 2013; Luo *et al.* 2019; Shahvari *et al.* 2019).

The Soil & Water Assessment Tool (SWAT) (Arnold *et al.* 1998) is popularly used for large-scale hydrologic modeling. It simulates various hydrological cycle components under climate change scenarios (Chen *et al.* 2019; Ercan *et al.* 2020). The data derived from general circulation models (GCMs) under different greenhouse gas forcing scenarios are often used to analyze climate change impacts on the water resource availability and water supply systems (Krysanova & Hattermann 2017).

Vaghefi *et al.* (2015) coupled the SWAT with a water allocation model (MODSIM) to study climate change effects on cropping patterns in Iran's Karkheh River Basin. They concluded that the coupled SWAT–MODSIM program was more suitable for identifying adaptation options required by farmers and decision-makers to respond to changing water availability. Carvalho-Santos *et al.* (2017) used a SWAT model to evaluate the suitability of a single- or two-reservoir system for water supply under climate change conditions in the Alto Sabor watershed in Portugal. They found that the reservoir water storage will decrease under climate change conditions. Also, a two-reservoir system will have less reliability to supply water in the future. Fereidoon & Koch (2018) used a coupled simulation–optimization tool, SWAT–LINGO–MODSIM–PSO (SLMP), to determine optimal crop patterns for the Karkheh River Basin in Iran under climate change. They concluded that the SLMP model could serve as a practical tool to analyze the agricultural benefits under climate change impacts.

Kangrang *et al.* (2019) investigated the optimal reservoir rule curve for future climate change in the Ubolrat Basin in Thailand. They used a methodology that used a SWAT

model, a coupled genetic algorithm, and a reservoir mathematical model. They found that the new rule curve's performance was better than the old rule in the climate change condition. Ahmadianfar & Zamani (2020) assessed the performance of the Jarreh reservoir in Khuzestan province in Iran under climate change conditions. They adapted the reservoir operation policy based on reservoir inflow variation under climate change conditions. They concluded that the reservoir performance and water resource management would be more reliable based on their operation policy. According to the previous studies, reservoir performance evaluation to supply water is an essential issue under climate change.

The Zayandeh-Roud Basin is one of the most critical basins in Iran, located in a semi-arid area. Erratic precipitation patterns, uneven distribution of the water resources, repeated prolonged droughts, and human factors in the region have led to considerable challenges for water availability and supply across the river basin. The multipurpose Zayandeh-Roud Reservoir with a storage capacity of 1.5 MCM (SWRC 2009) regulates the river flow. It supplies water during drought or water shortage. The reservoir inflow has considerably reduced in recent years (Figure 1), posing significant water availability problems for the various regional uses. According to the variation of water demands in different sectors and impacts of climate change, the water supply condition may become critical. The majority of the previous studies assessed the effects of climate change on the meteorological and hydrological components of catchments and optimized the benefits of the agricultural sector in the future. However, no study optimized water allocations to other water users besides the agricultural sector under climate change, along with considering the possible changes in different water demands. Most climate change studies on this region also used the third and fourth reports of IPCC (Intergovernmental Panel on Climate Change) scenarios.

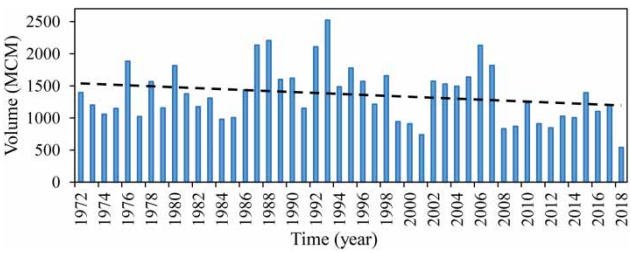

Figure 1 | Total flow volume entering the Zayandeh-Roud Reservoir up to the year 2018.

In the present study, the impacts of climate change on the reservoir inflow and meteorological components were investigated using ISI-MIP5 (Inter-Sectoral Impact Model Intercomparison Project) GCMs. In addition, the allocation of available water to agricultural, industrial, and domestic sectors was optimized regarding possible changes in the future water demands.

This study aimed to quantify the expected impacts of climate change in the future. Furthermore, the study was carried out to optimize water allocations by minimizing water deficits in the agricultural, industrial, and domestic sectors. To achieve these objectives, a SWAT model of the study area was built in both historical and future periods. The simulated reservoir inflow under climate change scenarios was used to optimize water distribution in the future.

To model the impact of climate change, we used five ISI-MIP5 GCMs: GFDL-ESM2Mt, HadGEM2-ES, IPSL-CM5A-LR, MIROC, and NoerESM1-M under four Representative Concentration Pathways (RCPs): RCP2.6, RCP4.5, RCP6.0, and RCP8.5. A nonlinear optimization model was applied to minimize the water deficits while also appropriately responding to agricultural, industrial, and domestic demands. The optimization problem was solved in the LINGO software. The reservoir performance was evaluated based on two indices: reliability and vulnerability.

STUDY AREA

The study area is upstream of the Zayandeh-Roud Reservoir (49°50′–50°40′E and 32°20′–33°10′ N), located in the Zayandeh-Roud River Basin in central Iran. It covers an area of around 4,100 km^2 (Figure 2). The study area is climatically and hydrologically different from the rest of the basin because of the high elevation. It receives annual precipitation of around 1,400 mm. The Zayandeh-Roud River is the most crucial surface flow in the basin. It supplies water for agriculture, industry, domestic, and other household purposes in Isfahan and Chaharmahal and Bakhtiari provinces in central Iran. The existence of high-flow rivers in the neighboring basins, such as Chaharmahal and Bakhtiari, has encouraged inter-basin water transfer projects to supply part of the water

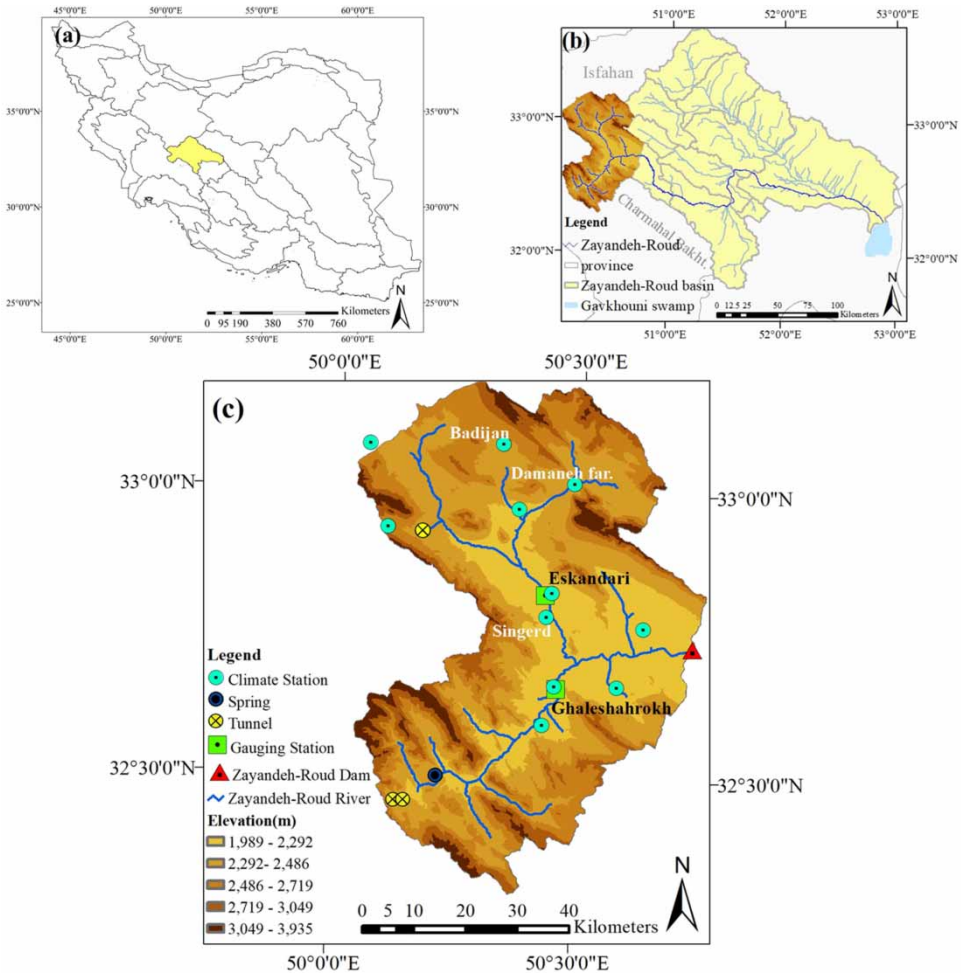

Figure 2 | (a) Iran, (b) Zayandeh-Roud Basin, and (c) upstream of the Zayandeh-Roud Reservoir study area.

shortage in the Zayandeh-Roud River Basin. There are three tunnels in the study area for this purpose.

DATA AND METHODS

A conceptual modeling approach

The SWAT was used to build a hydrologic model of the study area. Calibration/validation, sensitivity analysis, and uncertainty analysis were performed using the SUFI-2 algorithm (Abbaspour *et al.* 2007). Data derived from five GCMs were used to compute the variations in precipitation and temperature as well as their effects on the reservoir inflow. Finally, optimal water allocations of the reservoir to different uses were determined for future periods using the LINGO software. A schematic plot of the study process is shown in Figure 3.

SWAT model setup and input data

The SWAT is a process-based, semi-distributed, continuous-time program and has an efficient computational simulator (Arnold *et al.* 2012). The river basin is initially divided into the smaller subbasins based on a digital elevation model (DEM). These subbasins are further divided into the hydrologic response units (HRUs) consisting of homogeneous units of land use, soil type, and slope (for more information, see Neitsch *et al.* 2011). The study region was divided into 45 subbasins and 405 HRUs using a 10% threshold for soil, 5% for land use, and 5% for slope. The thresholds were defined to

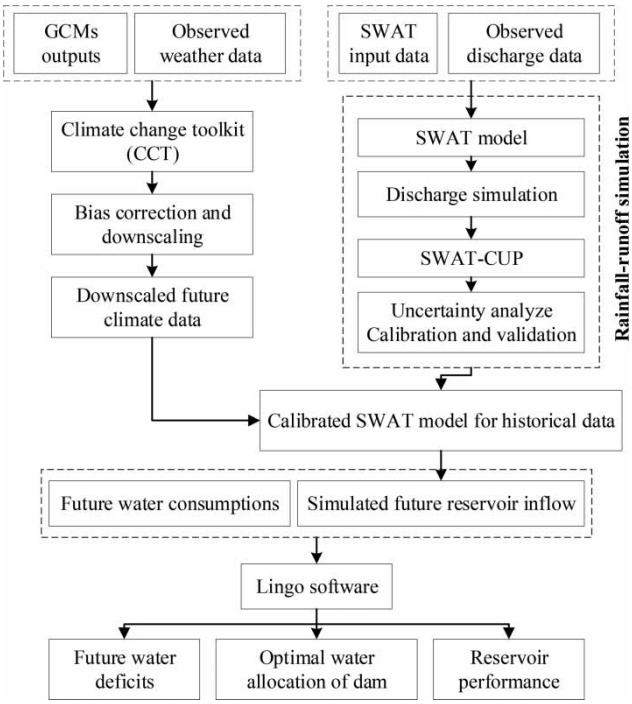

Figure 3 | Schematic plot of the study process.

eliminate small inconsequential units and to reduce the model calculation time. Data required to build the SWAT model and their sources are summarized in Table 1. There are three tunnels in this region, which transfer water from the adjacent basins to the study area. Monthly tunnel data were added to the streamflow in the SWAT model. In this study, the SWAT model was built from 1987 to 2015. The observed discharges from two stations, Ghaleshahrokh and Eskandari, were used to calibrate (1991–2008) and validate (2009–2015) the model with three years of the warm-up period (1987–1990).

Hydrological simulation

The SWAT model uses the Soil Conservation Service (SCS) curve number method developed by the SCS to simulate the runoff. The SCS curve number equation is:

$$Q_{\text{Surf}} = \frac{(R_{\text{day}} - I_a)^2}{(R_{\text{day}} - I_a + S)} \quad (1)$$

where Q_{Surf} is the accumulated runoff or rainfall excess (mmH_2O), R_{day} is the rainfall depth for the day (mmH_2O), I_a is the initial abstraction, which includes surface storage, interception, and infiltration before runoff (mmH_2O), and S is the retention parameter (mmH_2O). The retention parameter varies spatially due to changes in soils, land use, management, and slope and temporally due to changes in soil water content. The retention parameter is defined as:

$$S = 25.4\left(\frac{1000}{\text{CN}} - 10\right) \quad (2)$$

where CN is the curve number for the day. The initial abstractions I_a are commonly approximated as $0.2S$, and Equation (1) becomes:

$$Q_{\text{Surf}} = \frac{(R_{\text{day}} - 0.2S)^2}{(R_{\text{day}} + 0.8S)} \quad (3)$$

The runoff will only occur when $R_{\text{day}} > I_a$. The steps of SWAT runoff simulation are summarized in Figure 4. The

Table 1 | Data description and sources

Data type	Time period	Resolution/detail	Source
DEM map	2008	50×50 m	IRWA
Soil map	2009	47 types	IRWA
Land-use map	2005	1:250,000	IRWA
Discharge	1987–2015	Two stations	IRWA
Precipitation	1987–2015	Rain gauge	IRWA
Precipitation and temperature (max. and min.)	1987–2015	Evapotranspiration gauge	IRWA
Precipitation and temperature (max. and min.)	1987–2015	Climatology	IMO
Precipitation and temperature (max. and min.)	1987–2015	Synoptic	IMO
Reservoir outflow	1991–2015	Zayandeh-Roud Reservoir	IRWA
Inter-basin water transfer (inflow to the Basin)	1990–2015	Tunnels	IRWA
Agricultural management	1990–2015	Plant, harvest, cropping pattern	IAJO
Consumptive water use	1990–2015	Industrial and municipal	IRWA

IRWA, Isfahan Regional Water Authority; IMO, Iranian Meteorological Organization; IAJO, Isfahan Agricultural Jahad Office.

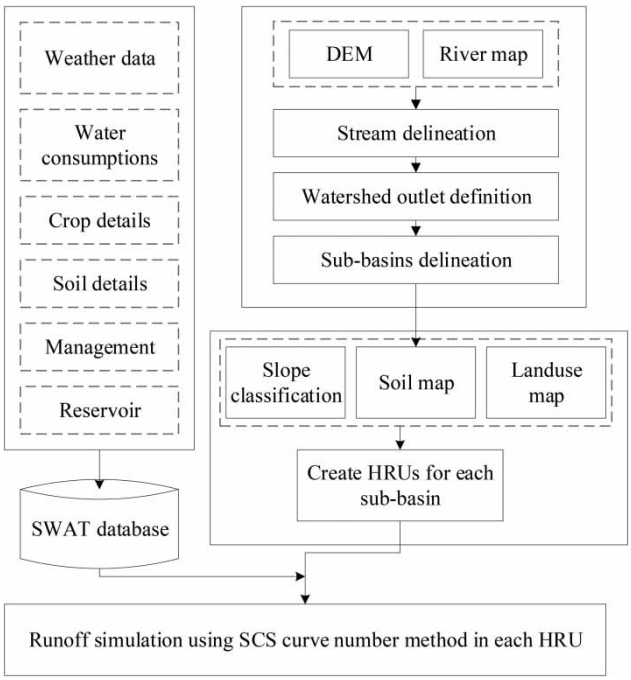

Figure 4 | The steps of SWAT runoff simulation.

SWAT model's automatic irrigation option was used for agricultural management and dividing the agricultural land uses into different crops. The data obtained from the Isfahan Agricultural Jahad Office on the cropping patterns in the townships across the Zayandeh-Roud River Basin were used to assign the irrigated crops. Given that the cropping patterns in the basin were diverse, the area under each crop was initially used to determine the predominant crop(s) in each township. The land-use maps, township boundary maps, and boundary maps of the subbasins constructed in the ArcSWAT model were then used to assign predominant crops to each SWAT subbasin in the model by the Geographic Information System. Ultimately, wheat, barley, alfalfa, rice, potato, and corn were identified as the dominant crops.

Future meteorological data and climate change scenarios

Data from GFDL-ESM2Mt, HadGEM2-ES, IPSL-CM5A-LR, MIROC, and NoerESM1-M models, and four RCPs such as RCP2.6, RCP4.5, RCP6.0, and RCP8.5 were used to simulate the climate data for the years 2020–2045 at four climate stations: Badijan, Ghaleshahrokh, Damanehfereidan, and Singerd (Figure 2).

The bias correction and downscaling of the GCM outputs were performed in the Climate Change Toolkit (CCT) software for the historical period (1981–2006) based on the following equations (Vaghefi *et al.* 2017):

$$T_{\text{corrected}_{ij}} = T_{\text{GCM}_{ij}} + (\bar{T}_{\text{refrence}_{jk}} - \bar{T}_{\text{GCM}_{jk}}) \quad (4)$$

$$P_{\text{corrected}_{ij}} = P_{\text{GCM}_{ij}} \times \left(\frac{\bar{P}_{\text{refrence}_{jk}}}{\bar{P}_{\text{GCM}_{jk}}}\right) \quad (5)$$

where $T_{\text{GCM}_{ij}}$ is the temperature projected by GCMs, $\bar{T}_{\text{refrence}_{jk}}$ is the measured temperature, $\bar{T}_{\text{GCM}_{jk}}$ is the average temperature projected by GCMs, $P_{\text{GCM}_{ij}}$ is the precipitation projected by GCMs, $\bar{P}_{\text{refrence}_{jk}}$ is the average measured precipitation, $\bar{P}_{\text{GCM}_{jk}}$ is the average projected precipitation by GCMs, $T_{\text{corrected}_{ij}}$ is the temperature corrected by the CCT, and $P_{\text{corrected}_{ij}}$ is the precipitation corrected by the CCT. Subscripts i, j, and k stand for the day, month, and year, respectively.

There are different uncertainties in GCM outputs that affect the reliability of future projection. Using different climate change scenarios produced by multiple GCMs could represent more accurate future climate data. Single GCM can be less reliable and include more uncertainties (Lee *et al.* 2011). Multimodel projections can be categorized as equally probable projections and weighted projections. In the first category, each component of the ensemble models is assumed to represent an equal probability of future conditions. In the second category, the models are weighted based on their ability to reproduce the observed climate variables. In this study, each GCM was weighed based on its historical period (1981–2006) performance compared to the observed climate data. The weights were calculated using the following equations (Gohari *et al.* 2013):

$$W_i = \frac{\left(\frac{1}{\Delta T_i}\right)}{\sum_{i=1}^{N}\left(\frac{1}{\Delta T_i}\right)} \quad (6)$$

$$W_i = \frac{\left(\frac{1}{\Delta P_i}\right)}{\sum_{i=1}^{N}\left(\frac{1}{\Delta P_i}\right)} \quad (7)$$

where W_i is the weight of each model in the ith month, ΔT is the long-term mean deviation of temperatures simulated by the GCMs over the base period, and ΔP is the long-term mean deviation of simulated precipitations.

Optimal water allocation of the reservoir

The following optimization model was proposed for minimizing the sum of squares shortage between the water demand and release throughout the future period defined as:

$$\text{Min}F = \sum_t^T \left(\frac{R_t - D_t}{D_t}\right)^2 \text{ for } t = 1, 2, \ldots, T \quad (8)$$

where R_t and D_t represent the total water release for three sectors (agriculture, industry, and domestic) and the total demand in each month, respectively. First, the total release was optimized based on minimizing the total water deficits in all sectors; then, the available water was allocated based on the priorities of each sector. The prioritization was proportioned based on the average water each sector had received during the base period.

The continuity equation that provides the water balance during the reservoir operation period and two constraints on the monthly release and reservoir storage are defined as:

$$S_{t+1} = S_t + I_t + P_t - E_t - R_t - \text{loss}_t \quad \text{for } t = 1, 2, \ldots, T \quad (9)$$

$$\text{subject to: } 0 < R_t < D_t,\ S_{\min} < S_t < S_{\max} \quad \text{for } t = 1, 2, \ldots, T \quad (10)$$

where S_{t+1} is the volume of water stored at the end of each month, S_t is the water storage at the beginning of each month, P_t is the volume of monthly precipitation on the reservoir, E_t is the volume of monthly evaporation, R_t is the volume of monthly water release, I_t is the monthly reservoir inflow volume, and loss_t is the monthly volume of water lost from the reservoir bed (Neitsch *et al.* 2011).

To evaluate the reservoir performance, the reliability and vulnerability indices were used, which are calculated based on the following equations (Hashimoto *et al.* 1982).

Reliability index

The reliability index was defined as the probability that the available water of the system meets the demands during the operation period (satisfactory state):

$$R_e = \frac{N_{t=1}^n (D_t \le R_t)}{n} \quad t = 1, 2, 3, \ldots, n \quad (11)$$

where R_e is the reliability index, $N_{t=1}^n (D_t \le R_t)$is the number of times that a system is in a satisfactory state, R_t and D_t are water release and demand, respectively, and n is the total number of states.

Vulnerability index

The vulnerability index indicates the magnitude of the reservoir operation failures:

$$V_u = \frac{\sum_{t=1}^{n} (D_t - R_t)}{\sum_{t=1}^{n} D_t} \quad t = 1, 2, \ldots, T \quad (12)$$

where V_u is the vulnerability over the T period, R_t and D_t represent water release and demand, respectively.

Estimation of future water demands

Due to the imbalance between water availability and water consumption, the current policy based on the State Water Master Plan (SWMP) report increases irrigation while keeping the current area of agricultural lands constant (SWMP 2012). Also, the domestic water supply was estimated based on population growth. The following water needs were estimated based on the report provided by the SWMP.

Agricultural demand

The gross agricultural water need in the future was calculated based on the cultivated areas during 2016–2045. The total cultivated area was considered constant and equal to the areas reported in the SWMP for the base period. The total future gross water demand was calculated based on the past net demand and the projected agricultural

efficiency provided by the SWMP report for 2041. According to the SWMP report, 30% of the gross agricultural demand is supplied by the reservoir. The remaining is supplied by other sources such as groundwater.

Industrial demand

According to the SWMP report, the industrial demand supplied by the surface waters in the base period is 112 MCM/year. In this study, the industrial demand was assumed to remain the same.

Domestic demand

The population living in regions whose domestic demands depended on the Zayandeh-Roud Reservoir was estimated to be 4,736,628 by 2041. Based on the average daily per capita water consumption of 267 litres, the domestic sector's future annual demand was estimated to be around 490 MCM/year (SWMP 2012).

Model calibration, sensitivity, and uncertainty analysis

For calibration and validation of the model based on measured runoff, the SUFI-2 algorithm in the SWAT-CUP software was used. This program also calculates parameter sensitivity and model uncertainty. Model prediction uncertainty accounts for all modeling errors (e.g., model parameters, observation data, and conceptual model) (Abbaspour *et al.* 2007). Propagation of the uncertainties in the parameters leads to uncertainties in the model output variables, expressed as the 95% prediction uncertainty (95PPU), computed at 2.5 and 97.5% levels of the cumulative distribution of an output variable. The *p*-factor and *r*-factor are two criteria used to measure the goodness of fit and model uncertainty, respectively. The *p*-factor is the percentage of observed data bracketed by the 95PPU band. Simultaneously, the *r*-factor is the average thickness of the 95PPU band divided by the standard deviation of observation data. The ideal values of the *p*-factor and *r*-factor are 100 and 0%, respectively, indicating a perfect match between the observed and simulated values. The objective in this process is, therefore, to obtain a high *p*-factor with a small *r*-factor. Abbaspour *et al.* (2015) suggested that for flow, values of >0.7 for *p*-factor and <1.5 for *r*-factor constitute a good calibration result.

The Nash–Sutcliffe efficiency (NSE) was used as the measure of goodness of fit and formulated the following objective function:

$$\mathrm{NSE} = 1 - \frac{\sum_{i=1}^{n} (Q_{\mathrm{si}} - Q_{\mathrm{oi}})^2}{\sum_{i=1}^{n} (Q_{\mathrm{oi}} - \bar{Q}_{\mathrm{oi}})^2} \tag{13}$$

where Q_{si} is the simulated discharge, Q_{oi} is the observed discharge, and $\bar{Q}_{\mathrm{oi}}$ is the mean value of the observed discharge. If there is more than one variable, then the objective function is calculated as:

$$g = \frac{1}{\sum w_i} \sum_i w_i \mathrm{NSE} \tag{14}$$

where w_i is the weight of the ith variable. In this study, it was assumed that the weight for each station is to be equal to 1. So, the objective function value is the average NSE of the two stations.

Parameter sensitivities were determined by calculating the following multiple regression system, which regresses the parameters against the objective function values:

$$g = \alpha + \sum_{i=1}^{m} \beta_i b_i \tag{15}$$

A *t*-test was then used to identify the relative significance of each parameter b_i. The sensitivities given above are estimates of the average changes in the objective function resulting from changes in each parameter while all other parameters change. This gives relative sensitivities based on linear approximations and only provides partial information about the objective function's sensitivity to model parameters. In this analysis, the larger, in absolute value, the value of *t*-stat, and the smaller the *p*-value, the more sensitive the parameter (Abbaspour *et al.* 2017a).

RESULTS AND DISCUSSION

Sensitivity analysis

A large number of parameters were initially selected for the sensitivity analysis. In the end, seven hydrologic parameters were sensitive to discharge at the 95% confidence level. The most sensitive parameters were CN2, followed by GWQMN, GW_REVAP, and RCHRG_DP (Table 2). Initially, the five snow parameters were calibrated and removed from further calibration to avoid identifiability problems with the other hydrologic parameters (Abbaspour *et al.* 2017a). The snowmelt base temperature (°C) (SUB_SMTM) was the most sensitive snow parameter.

Calibration and validation

For the calibration period, a *p*-factor of 0.79 at the Ghaleshahrokh station was obtained (Figure 5(a)), which means the 95PPU bracketed 79% of the observed data. The *r*-factor was 1.01, indicating an acceptable uncertainty level for discharge. For the Eskandari station (Figure 5(b)), a *p*-factor of 0.70 and an *r*-factor of 0.60 were obtained. The model prediction was less uncertain at the Eskandari station; however, it bracketed less observed data, indicating a slightly larger simulation error (=1 – *p*-factor) for small flow conditions, as also observed before by Abbaspour *et al.* (2015). The NSE values for the 'best' parameter set, i.e., the parameter set with the highest objective function value, were 0.75 and 0.61 for the Ghaleshahrokh and Eskandari stations, respectively. However, as the hydrologic model results are inherently uncertain because of unavoidable errors in the input data, the *p*-factor and the *r*-factor better describe a model's calibration reliability. All post-processings using a calibrated model must propagate the calibrated parameter ranges to obtain model prediction uncertainty and avoid using the 'best' parameter set only (Abbaspour *et al.* 2017b).

Similarly, acceptable results were obtained for the validation, which had similar climatic and hydrologic conditions as the calibration period. For the Ghalehshahrokh station (Figure 5(c)), the *p*-factor was 0.71, and the *r*-factor was 0.70. These values for the Eskandari station (Figure 5(d)) were 0.72 and 0.67, respectively.

Effects of climate change on precipitation and temperature

The variations in mean annual temperature during the period of 2020–2045 exhibited an increasing trend from

Table 2 | Ultimate actual ranges of sensitive parameters to discharge

	Parameter	Parameter definition	Actual ultimate range/fixed value	*t*-stat	*p*-value
1	[a]r__CN2.mgt	SCS runoff curve number	66.5–82.2	20.5	0
2	v__GWQMN.gw	Threshold depth of water in shallow aquifer for return flow (mm)	0.00–417	−5.5	0
3	v__GW_REVAP.gw	Groundwater revap. coefficient	0.08–0.1	−3.8	0.0001
4	v__RCHRG_DP.gw	Deep aquifer percolation fraction	0.36–0.5	3.0	0.003
5	v__ESCO.hru	Soil evaporation compensation factor	0.90–1	2.8	0.004
6	v__SHALLST.gw	Initial depth of water in the shallow aquifer (mm)	1,337–2,000	2.4	0.01
7	r__SOL_AWC.sol	Soil available water storage capacity ($mmH_2O/mmsoil$)	0.11–0.16	−2.2	0.02
8	v_SFTMP.sno	Snowfall temperature (°C)	1.3	–	–
9	v_SMTMP.sno	Snowmelt base temperature (°C)	0.5	–	–
10	v_SMFMX.sno	Maximum melt rate for snow during the year ($mm\ C^{-1}day^{-1}$)	4.5	–	–
11	v_SMFMN.sno	Minimum melt rate for snow during the year ($mm\ C^{-1}day^{-1}$)	5.1	–	–
12	v_TIMP.sno	Snowpack temperature lag factor	0.5	–	–

[a] r__ indicates relative change, and v__ indicates value change.

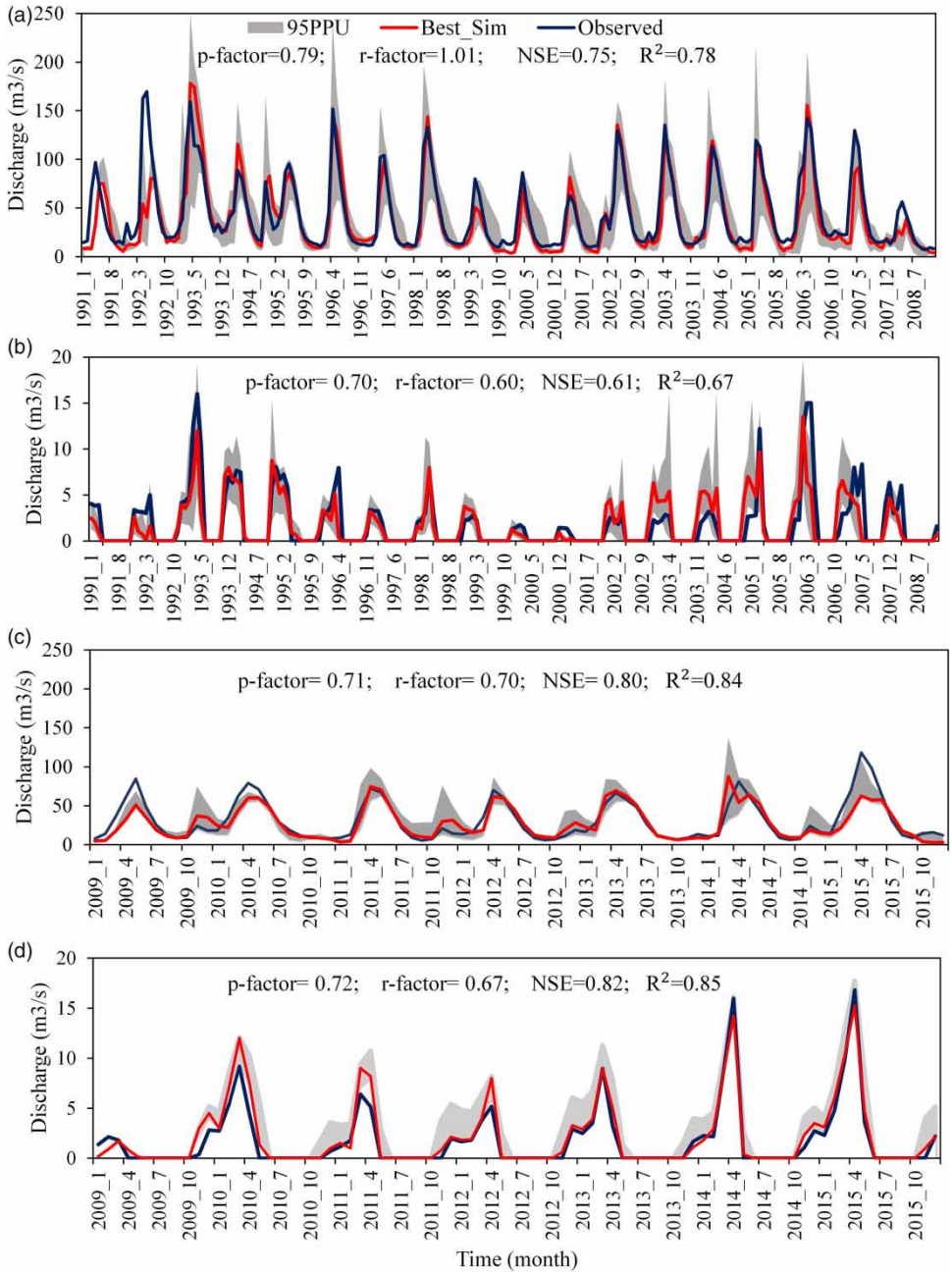

Figure 5 | Discharge calibration results for the period of 1991–2008 at (a) the Ghalehshahrokh station and (b) the Eskandari station. Discharge validation results for the period of 2009–2015 at (c) the Ghalehshahrokh station and (d) the Eskandari station.

19.9% (1.8 °C) in RCP2.6 to 29.4% (2.7 °C) in RCP8.5 compared to the base period (Table 3). In the future, mean annual precipitation is projected to decline under all the region scenarios, with the maximum reduction of 8.2% (32.8 mm) expected to occur under RCP8.5.

Effects of climate change on the Zayandeh-Roud Reservoir inflow volumes

The SWAT model results indicated reductions of 41–51% inflow volumes relative to the average volumes in the base

Table 3 | Regionalized mean annual temperature and cumulative precipitation for the base and future periods

Scenario	Regionalized precipitation (mm)	Variation (%)	Regionalized temperature (°C)	Variation (%)
Base period	398.6	–	9.5	–
RCP2.6	391.9	−1.7	11.3	18.9
RCP4.5	398.1	−0.1	11.8	24.2
RCP6.0	390.6	−2.0	11.9	25.9
RCP8.5	365.8	−8.2	12.2	28.4

period under the different scenarios (Table 4). The highest percentage variation was projected to occur under RCP8.5, indicating the most severe radiative forcing in the future.

Optimal water allocation of the reservoir under climate change

The upper and lower limits of the monthly reservoir storage volume were 1,400 and 120 MCM, respectively. In addition, the initial dam storage volume was assumed to be equal to 260 MCM, and the last dam storage was the same as the initial storage. The maximum and minimum of optimized water release were under RCP2.6 and RCP8.5 in all months, respectively (Figure 6). Based on the water allocation priority mentioned in the 'Optimal water allocation of the reservoir' section, the amount of water released under both scenarios completely satisfied the domestic and industrial water demands even in the dry months (March–August). At the same time, the agriculture sector did not receive its full demand even under the RCP2.6 with the highest water release over the projection period (Figure 7).

The water deficits will probably persist due to climate change under all the scenarios and throughout all months (Figure 8(a)). The highest water shortage is expected to

Table 4 | Mean annual of total reservoir inflow during the base and future periods

Scenario	Mean annual of total reservoir inflow (MCM)	Variation (%)
Base period	1,233	–
RCP2.6	723	−0.41
RCP4.5	672	−0.45
RCP6.0	696	−0.44
RCP8.5	607	−0.51

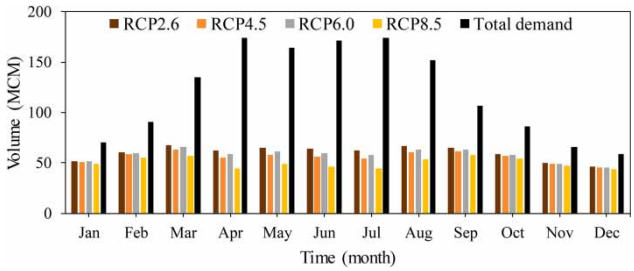

Figure 6 | Monthly average of the optimized release in the period (2020–2045) under the four climate change scenarios.

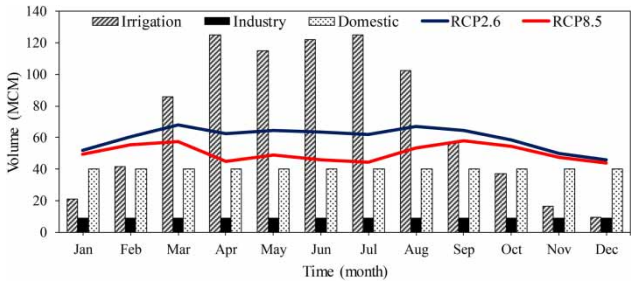

Figure 7 | Monthly average of the water demand and the total allocated water over the period of 2020–2045.

occur in the dry months (March–August) under all scenarios. Also, the highest irrigation demand belongs to these months. Therefore, it is evident that the demand at its peak in these months could contribute to increasing water shortage and adversely affect crop yield. Moreover, mean annual water deficits in the future years will vary between 730 and 847 MCM, with the highest and the lowest estimated to occur under RCP8.5 and RCP2.6, respectively (Figure 8(b)).

Reservoir performance indices due to climate change impacts

The lowest reliability index of 0.6% and the highest vulnerability index of 59% are related to RCP8.5 compared to other scenarios (Table 5). The present results obtained for the reservoir performance under RCP8.5 agreed with those obtained in the previous sections showing the highest water deficit for this scenario. Overall, the agricultural sector's water shortages will affect the overall reservoir performance and make it unreliable and vulnerable in the future.

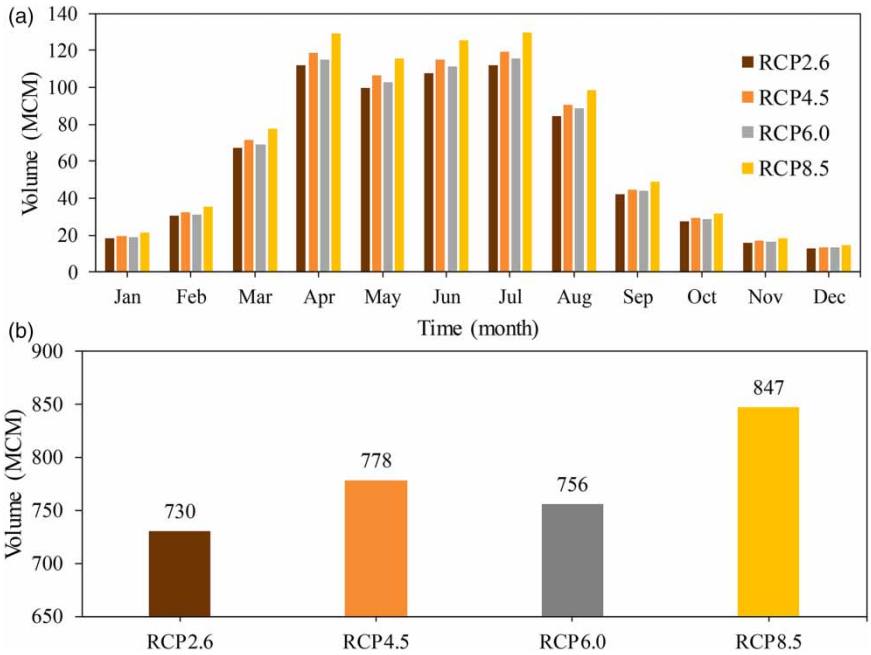

Figure 8 | (a) Monthly average of total water deficits and (b) annual average of total water deficits under four climate change scenarios over the period of 2020–2045.

Table 5 | Performance indices for meeting 80% of the demand under climate change impacts

Scenario	Reliability (%)	Vulnerability (%)
RCP2.6	3	50
RCP4.5	2	53
RCP6.0	4.6	52
RCP8.5	0.6	59

Model uncertainty and limitations

The study limitations are partly due to the assumptions that (i) the effect of climate change was evaluated based on four meteorological stations, (ii) the optimal water allocation was investigated based on the water demands that are supplied by the reservoir and the water demands which, supplied by groundwater, were not considered, and (iii) the water demands were calculated based on the projection of the SWMP report. Climate change affects the crop water demand, which should be considered in future studies. Other study limitations are the general errors of large-scale modeling, assumptions, and data limitation, especially on the agricultural management and management of the rivers and the reservoir.

Several sources of uncertainty in the reservoir operation include climate data, projected reservoir inflow, and catchment characteristics, which were considered in the hydrological modeling and climate change analysis. Hydrological models suffer from several sources of uncertainty, such as the conceptual model, input data, model parameters, and observation data. In this study, the SUFI-2 algorithm was used for the model calibration/validation, which accounts for all model uncertainties. The uncertainty of GCM outputs was considered by assigning weight to the GCMs based on their historical period performance. Other sources of uncertainty can be examined in future research.

CONCLUSIONS

In this study, we assessed the impacts of climate change and the future performance of the Zayandeh-Roud Reservoir in Iran. The results showed that climate change would likely affect regional precipitation and temperature and significantly reduce the reservoir inflow. Due to the water allocation priority of domestic and industrial sectors over agricultural, the latter sector will face significant water shortages under climate change conditions. The awareness

of water availability in the future periods by considering both climate change impacts and variations in the demands in different sectors across the basin provides a better picture of water resource reliability. This realization should help water managers with the planning of future water structures.

DATA AVAILABILITY STATEMENT

All relevant data are included in the paper or its Supplementary Information.

REFERENCES

Abbaspour, K. C., Yang, J., Maximov, I., Siber, R., Bogner, K., Mieleitner, J., Zobrist, J. & Srinivasan, R. 2007 Modelling hydrology and water quality in the pre-alpine/alpine Thur watershed using SWAT. *Journal of Hydrology* **333** (2–4), 413–430. https://doi.org/10.1016/ j.jhydrol.2006.09.014.

Abbaspour, K. C., Faramarzi, M., Ghasemi, S. S. & Yang, H. 2009 Assessing the impact of climate change on water resources in Iran. *Water Resource Research* **45** (10). https://doi.org/10.1029/ 2008WR007615.

Abbaspour, K. C., Rouholahnejad, E., Vaghefi, S. A., Srinivasan, R., Yang, H. & Klove, B. 2015 A continental-scale hydrology and water quality model for Europe: calibration and uncertainty of a high-resolution large-scale SWAT model. *Journal of Hydrology* **524**, 733–752. https://doi.org/10.1016/ j.jhydrol.2015.03.027.

Abbaspour, K. C., Vaghefi, S. A. & Srinivasan, R. 2017a A guideline for successful calibration and uncertainty analysis for soil and water assessment: a review of papers from the 2016 International SWAT Conference. *Water* **10** (1), 6. https://doi.org/10.3390/w10010006.

Abbaspour, K. C., Kamali, B. & Yang, H. 2017b Assessing the uncertainty of multiple input datasets in the prediction of water resource components. *Water* **9** (9), 709. https://doi.org/10.3390/w9090709.

Ahmadianfar, I. & Zamani, R. 2020 Assessment of the hedging policy on reservoir operation for future drought conditions under climate change. *Climatic Change* **159** (2), 253–268. https://doi.org/10.1007/s10584-020-02672-y.

Arnold, J. G., Srinivasan, R., Muttiah, R. S. & Williams, J. R. 1998 Large area hydrologic modeling and assessment part I: model development 1. *JAWRA Journal of the American Water Resources Association* **34** (1), 73–89. https://doi.org/10.1111/j.1752-1688.1998.tb05961.x.

Arnold, J. G., Moriasi, D. N., Gassman, P. W., Abbaspour, K. C., White, M. J., Srinivasan, R., Santhi, C., Harmel, R. D., Van Griensven, A., Van Liew, M. W., Kannan, N. & Jha, M. K. 2012 SWAT: model use, calibration, and validation. *Transactions of the ASABE* **55** (4), 1491–1508. https://doi.org/10.13031/2013.42256.

Ashofteh, P. S., Haddad, O. B. & Loáiciga, H. A. 2015 Evaluation of climatic-change impacts on multiobjective reservoir operation with multiobjective genetic programming. *Journal of Water Resources Planning and Management* **141** (11), 04015030. https://doi.org/10.1061/(asce)wr.1943-5452.0000540.

Carvalho-Santos, C., Monteiro, A. T., Azevedo, J. C., Honrado, J. P. & Nunes, J. P. 2017 Climate change impacts on water resources and reservoir management: uncertainty and adaptation for a mountain catchment in northeast Portugal. *Water Resources Management* **31** (11), 3355–3370. https://doi.org/10.1007/s11269-017-1672-z.

Chen, Y., Marek, G. W., Marek, T. H., Moorhead, J. E., Heflin, K. R., Brauer, D. K., Gowda, P. H. & Srinivasan, R. 2019 Simulating the impacts of climate change on hydrology and crop production in the Northern High Plains of Texas using an improved SWAT model. *Agricultural Water Management* **221**, 13–24. https://doi.org/10.1016/j.agwat.2019.04.021.

Ercan, M. B., Maghami, I., Bowes, B. D., Morsy, M. M. & Goodall, J. L. 2020 Estimating potential climate change effects on the upper neuse watershed water balance using the SWAT model. *JAWRA Journal of the American Water Resources Association* **56** (1), 53–67. https://doi.org/10.1111/1752-1688.12813.

Faramarzi, M., Abbaspour, K. C., Vaghefi, S. A., Farzaneh, M. R., Zehnder, A. J., Srinivasan, R. & Yang, H. 2013 Modeling impacts of climate change on freshwater availability in Africa. *Journal of Hydrology* **480**, 85–101. https://doi.org/10.1016/j.jhydrol.2012.12.016.

Fereidoon, M. & Koch, M. 2018 SWAT-MODSIM-PSO optimization of multi-crop planning in the Karkheh River Basin, Iran, under the impacts of climate change. *Science of the Total Environment* **630**, 502–516. https://doi.org/10.1016/j.scitotenv.2018.02.234.

Gohari, A., Eslamian, S., Abedi-Koupaei, j., Massah Bavani, A., Wang, D. & Madani, K. 2013 Climate change impacts on crop production in Iran's Zayandeh-Rud River Basin. *Science of the Total Environment* **442**, 405–419. https://doi.org/10.1016/j.scitotenv.2012.10.029.

Hashimoto, T., Stedinger, J. R. & Loucks, D. P. 1982 Reliability, resiliency, and vulnerability criteria for water resource system performance evaluation. *Water Resources Research* **18** (1), 14–20. https://doi.org/10.1029/WR018i001p00014.

Kangrang, A., Prasanchum, H. & Hormwichian, R. 2019 Active future rule curves for multi-purpose reservoir operation on the impact of climate and land use changes. *Journal of Hydro-environment Research* **24**, 1–13. https://doi.org/10.1016/j.jher.2019.03.001.

Krysanova, V. & Hattermann, F. F. 2017 Intercomparison of climate change impacts in 12 large river basins: overview of methods and summary of results. *Climatic Change* **141** (3), 363–379. https://doi.org/10.1007/s10584-017-1919-y.

Lee, J., De Gryze, S. & Six, J. 2011 Effect of climate change on field crop production in California's Central Valley. *Climatic Change* **109** (1), 335–353. https://doi.org/10.1007/s10584-011-0305-4.

Luo, M., Liu, T., Meng, F., Duan, Y., Bao, A., Xing, W., Feng, X., De Maeyer, P. & Frankl, A. 2019 Identifying climate change impacts on water resources in Xinjiang, China. *Science of the Total Environment* **676**, 613–626. https://doi.org/10.1016/j.scitotenv.2019.04.297.

Marin, M., Clinciu, I., Tudose, N. C., Ungurean, C., Adorjani, A., Mihalache, A. L., Davidescu, A. A., Davidescu, Ş. O., Dinca, L. & Cacovean, H. 2020 Assessing the vulnerability of water resources in the context of climate changes in a small forested watershed using SWAT: a review. *Environmental Research* **184**, 109330. https://doi.org/10.1016/j.envres.2020.109330.

Neitsch, S. L., Arnold, J. G., Kiniry, J. R. & Williams, J. R. 2011 *Soil and Water Assessment Tool Theoretical Documentation Version 2009*. Texas Water Resources Institute, College Station, TX, USA.

Shahvari, N., Khalilian, S., Mosavi, S. H. & Mortazavi, S. A. 2019 Assessing climate change impacts on water resources and crop yield: a case study of Varamin plain basin, Iran. *Environmental Monitoring and Assessment* **191** (3), 134. https://doi.org/10.1007/s10661-019-7266-x.

State Water Master Plan (SWMP). 2012 *6th Report*, Ministry of Energy, Gavkhooni Basin, Iran.

Studies of Water Resources and Consumptions (SWRC). 2009 *Zayandab Consulting Engineers' Reports*, Isfahan Regional Water Authority, Zayandeh-Roud Basin, Iran.

Vaghefi, S. A., Mousavi, S. J., Abbaspour, K. C., Srinivasan, R. & Arnold, J. R. 2015 Integration of hydrologic and water allocation models in basin-scale water resources management considering crop pattern and climate change: Karkheh River Basin in Iran. *Regional Environmental Change* **15** (3), 475–484. https://doi.org/10.1007/s10113-013-0573-9.

Vaghefi, S. A., Abbaspour, N., Kamali, B. & Abbaspour, K. C. 2017 A toolkit for climate change analysis and pattern recognition for extreme weather conditions – Case study: California-Baja California Peninsula. *Environmental Modelling and Software* **96**, 181–198. https://doi.org/10.1016/j.envsoft.2017.06.033.

Vorosmarty, C. J., Green, P., Salisbury, J. & Lammers, R. B. 2000 Global water resources: vulnerability from climate change and population growth. *Science* **289** (5477), 284–288. https://doi.org/10.1126/science.289.5477.284.

First received 3 August 2020; accepted in revised form 11 January 2021. Available online 2 February 2021